

STUDY AND ANALYSIS OF THE MECHANISMS OF CRACK PROPAGATION IN MIXED MODE (I + II) IN ASSEMBLIES OF 3D REINFORCED COMPOSITES

M. Stackler^{1*}, D. Brancherie¹, Z. Aboura¹, J. Schneider²

¹Laboratoire Roberval, UMR-CNRS 6263, Université de Technologie de Compiègne, Centre de Recherches de Royallieu, BP 20529 - 60205 Compiègne cedex, France

²Snecma Villaroche, Rond point René Ravaud - Réau, F-77550 Moissy-Cramayel, France

*matthieu.stackler@utc.fr

Keywords: 3D composites, interlaminar fracture, mixed-mode, multi-instrumentation.

Abstract

This study deals with the delicate problem of delamination in assemblies of 3D composites. A methodology to precisely detect the moment of the initiation in Mode I, Mode II and Mixed Mode (I + II) is proposed. Given the complexity of the 3D architectures, the effect of the width of the specimens is also discussed. Finally, the parameters of the energetic criterion of Benzeggagh & al are identified in order to feed, in future work, finite element models.

1 Introduction

The advent of a new generation of composite materials with three-dimensional reinforcements (sewn, 3D orthogonal, 3D woven ...) predict great opportunities but also raise new scientific challenges. Indeed, the strengthening in the third direction enables a significant improvement in the interlaminar strength, which remains one of the main concerns with composite laminates. It also increases the damage tolerance and performance in the third direction.

However, assembly of such materials under the form of several layers, due to the requirements of the design, is inevitably submitted to the problems of interfacial held.

The object of this study is to approach the aspects of crack propagation in an assembly of 3D composites. The tormented architecture of the interfaces to assemble will disrupt inevitably the failure mechanisms.

This work proposes to analyze the cracking process of this type of assembly submitted to Mode I, Mode II and mixed mode. The tests methodologies used for the understanding of mechanisms involved will be presented. In addition to the scenarios of ruin, depending on the type of solicitation, this study will seek to identify the parameters of the energetic mixed-mode fracture criterion of Benzeggagh & al [1].

2 Materials and testing methods

2.1 Materials

The studied material is a composite carbon / epoxy reinforced 3D. Several widths of specimens being available, it was initially decided to investigate the influence of this parameter. The preliminary study concerns the DCB and ENF specimens for which a width of 20 mm will be compared to a width of 40 mm. The width of 20 mm is recommended by the literature [2]. The results will determine the MMB specimen geometry.

Materials are obtained by resin transfer molding on dry preform (RTM). All test pieces are composed of a stack of two plies of 5 mm thickness each. A 10 μ m Teflon insert is positioned between the two plies prior to injection in order to create a pre crack in the median plane of the specimens.

2.2 Specimens choice

To identify the parameters of the mixed mode criteria three types of specimens were selected:

Double Cantilever Beam specimen (DCB) : widely used to study crack propagation in mode I. This test is used to highlight the crack initiation and to follow its evolution. (cf Fig 1)

End Notched Flexure specimen (ENF) : widely used to study crack propagation in Mode II. This type of testing can reveal the crack initiation. (cf Figure 2)

Mixed Mode Bending specimen (MMB) proposed by Reeder & al. [3] : regardless the length of the crack, the MMB test provides a propagation at a constant mixed mode. The length variation of the lever of the test fixture is used to fix this mixed mode ratio. (cf Fig 3)

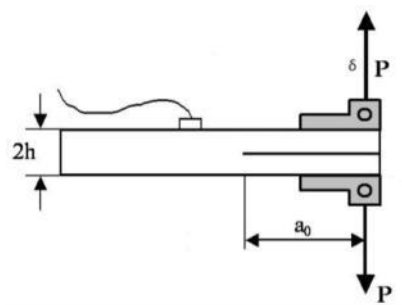


Figure 1. DCB specimen

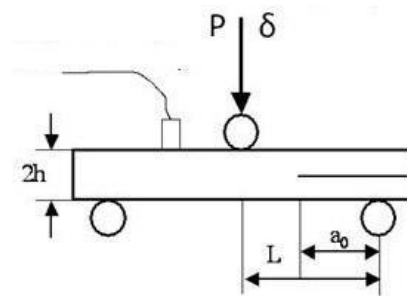


Figure 2. ENF specimen

	L (mm)	a_0 (mm)	B (mm)	h (mm)
DCB	~200	40 à 90	40	5
ENF	50	25	40	5
MMB	100	50 à 80	40	5

Tableau 1. specimens dimensions

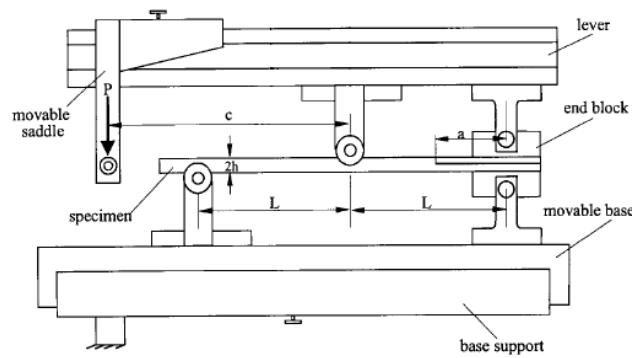


Figure 3. MMB test fixture

2.3 Instrument

The complexity of the material imposes an accurate instrumentation in order to robustly detect the crack initiation. Furthermore, this instrumentation will monitor the cracking process in real time during the test.

It consists of a high sensitivity camera for field measure, a strain gauge positioned at the crack tip, an acoustic emission sensor, a video microscope and sensors of load and displacement.

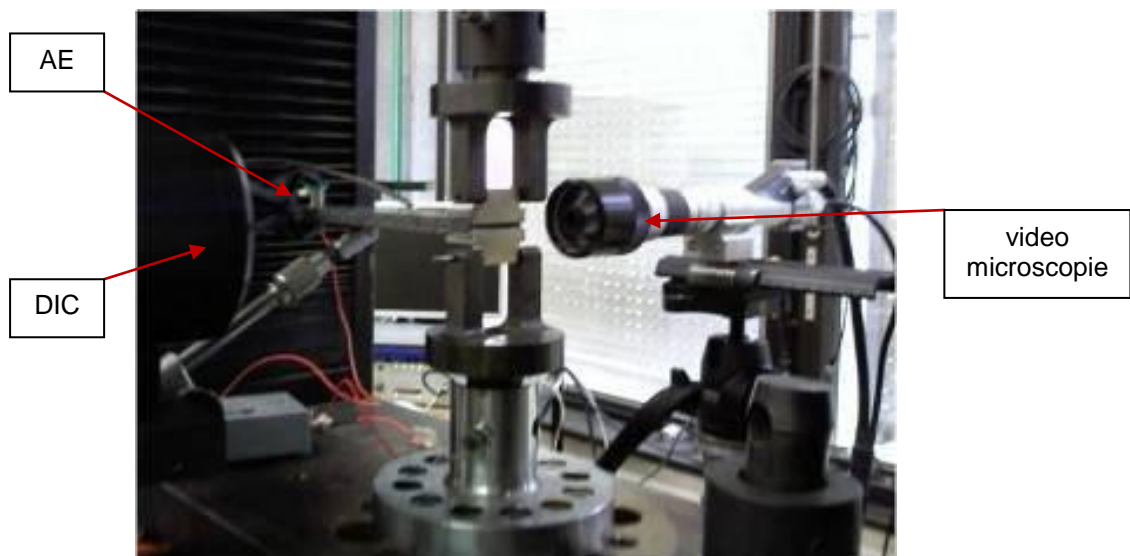


Figure 4. Multi-instrumented test fixture

The field measurement, allows to obtain an image of the strain variation on the edge of the specimen in the vicinity of the crack tip. The video microscopy a real-time tracking of the crack on the other side of the specimen. The acoustic emissions recording provides a global response of the phenomena that occur in the specimen (damage of the matrix, fiber / matrix failure or fiber breakage). Load and displacement recording allow to obtain a total value of the energy release rate depending on the evolution of the crack. Finally the strain gauge is used to display the time of initiation of the crack, its response will be correlated to field measured by DIC.

2.4 Data analysis

The measurement of energy release rate in mode I, will be based on the method of calibration of the compliance. For this, the specimens tested have precracking whose lengths vary from 40 to 90 mm. Compliance is expressed in two ways:

$$C = \frac{\delta}{P} \quad (1)$$

$$C = \frac{a^n}{h} \quad (2)$$

Where δ is the opening at the load application point, P is the load, a is the length of the precrack, n and h are the parameters of the empirical law proposed by Benzeggagh [4].

The energy release rate is obtained by the equation (3) :

$$G_I = \frac{1}{2B} \cdot P^2 \cdot \frac{na^{n-1}}{h} \quad (3)$$

Where B is the width of the specimen and P the corresponding load to the initiation of the crack.

The multi instrumentation has allowed us to highlight two interesting moments: the microscopic initiation and the macroscopic initiation. The first corresponds to a sharp increase in recording of acoustic emission (increase in the number of events and the energy of these events). The second is the visual opening of the crack and the first fall of load on load / displacement curve. (cf Fig 5 et 6) Between these two points, it remains an area particularly rich in mechanisms. The detailed analysis of this area is included in the prospects for this study.

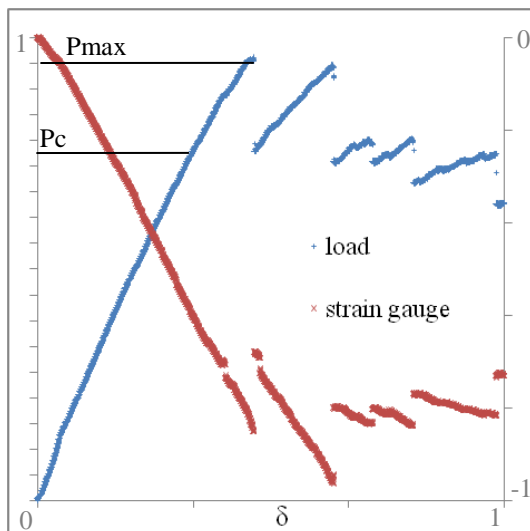


Figure 5. Evolution of the strength and deformation as a function of the opening at the load application point

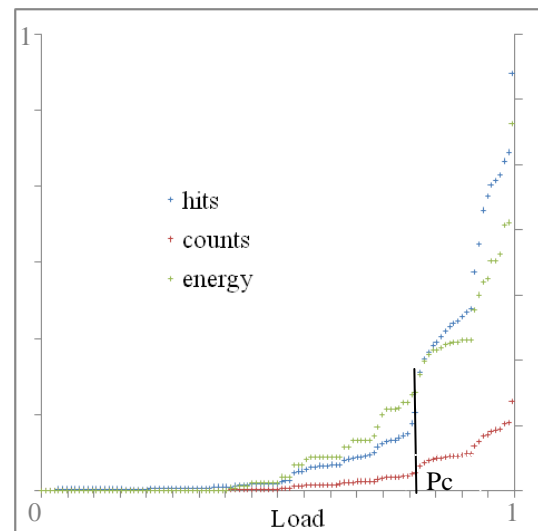


Figure 6. Evolution of acoustic emissions as a function of the applied load

The treatment of ENF tests does not require compliance calibration. Equation 4, based on beam theory, gives directly the energy release rate. The latter is obtained after measuring the initiation critical load.

$$G_{II} = \frac{9CP^2a^2}{2B(2L^2+3a^2)} \quad (4)$$

Where L is the half distance between the lower supports. C has the same expression as Equation 1, with δ the displacement of the load application point.

The ENF specimen is recommended to generate a sharp break, leaving no doubt for the determination of the critical load. However, there also appears a nonlinear region before a falling of load indicating the macroscopic initiation. Therefore we will also distinguish the microscopic and macroscopic initiations.

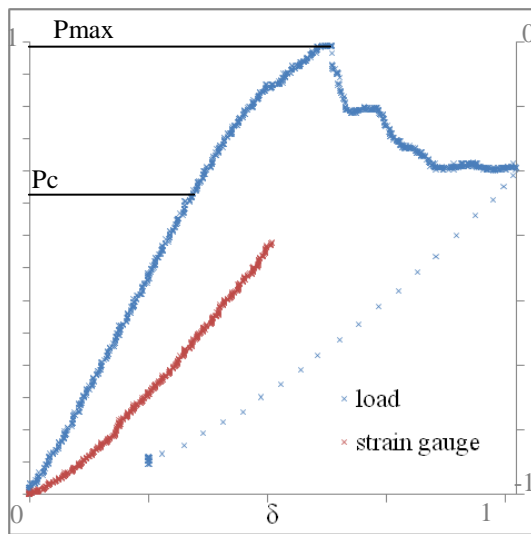


Figure 7. Evolution of the strength and deformation as a function of the opening at the load application point

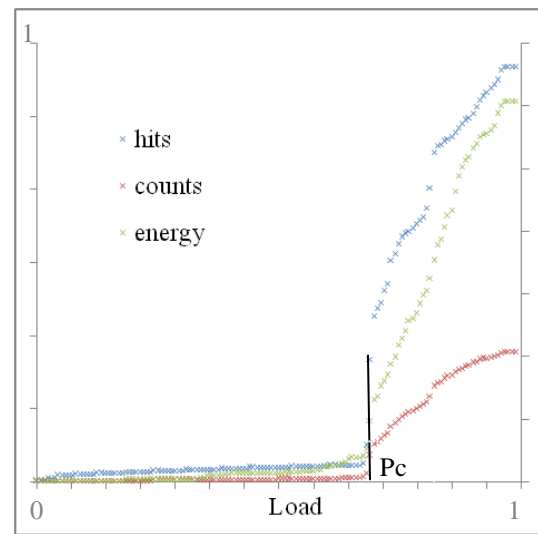


Figure 8. Evolution of acoustic emissions as a function of the applied load

The MMB tests are longer to implement, in effect they require compliance calibration for each modal ratio which will be tested to failure. The calibration consists of a series of tests where, for each modal ratio, Specimens with various precracking length are tested in their elastic range. Equation (5) is the semi-empirical expression of compliance in mixed mode [1]:

$$C = \alpha \cdot a^3 + \beta \quad (5)$$

Where α and β are parameters to be evaluated.

Once the point corresponding to the initiation is identified, Equation 6 gives the total energy release rate :

$$G_T = \frac{1}{2B} \cdot P^2 \cdot 3 \cdot \alpha \cdot a^2 \quad (6)$$

3 Results analysis

3.1 Mode I

The vast majority of cases dealt with in the literature, introduces results of tests in mode I carried out on specimens with a width approaching 20 mm. As mentioned above, it was decided to study the influence of specimen width on energy release rate average. For this, two sets of specimens were tested, the first with a width of 20 mm and the other with a width of 40 mm.

These tests demonstrate a difference of 11% of the energy release rate at the macroscopic initiation for specimens of 40 mm and decreased the standard deviation. The difference is not negligible, the following mode I tests were performed with the specimens of 40 mm.

During testing we noticed that the crack propagation is very jerky. This is illustrated by load jumps on the load / opening curve in Figure 5. These jumps are due to bifurcation of the crack in the resin rich areas. (cf fig 9) The crack moves from an interfacial zone to another crossing at 45 ° the resin rich clusters. This bifurcation remains confined to interplis.

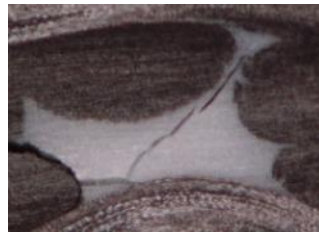


Figure 9. Bifurcation of the crack in an resin rich area

3.2 Mode II

As for DCB testing, ENF tests are mostly carried out on samples of 20 mm width. So we preceded to the same comparison on the width effect. The gap highlighted in these tests is lesser, it is 8% for specimens of 40 mm. These results confirms that obtained in mode I, the MMB tests performed following the DCB and ENF tests were realized on specimens of 40 mm.

3.3 Mixed Modes

Figures 10 and 11 show the typical curves of a MMB test. For these tests, the microscopic point of initiation appears quite clearly, this is the sharp increase of acoustic events and their energy. This point corresponds to the end of the linear part of the load / displacement curve. Unlike the DCB and ENF tests, the macroscopic initiation point is harder to determine. Photos of the sides taken at regular intervals during the test, and the results of image correlation, permit to determine it. What makes this initiation hard to detect, is that there is no significant point on the load and acoustic emission curves. On the load / displacement curve, the beginning of the portion between the end of the linearity and the maximum is due to plastic deformation of the crack front. The second part (after macroscopic initiation) corresponds to a propagation phase where the energy release rate is increasing.

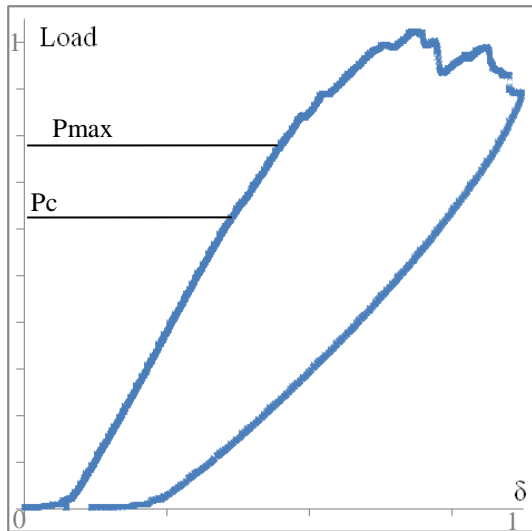


Figure 10. Evolution of load as a function of the displacement of the load application point

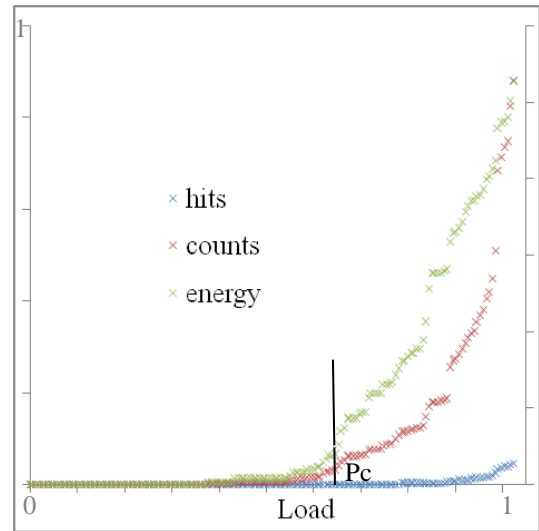


Figure 11. Evolution of acoustic emissions as a function of the applied load

The figure 12 shows the evolution of energy release rate as a function of the modal ratio. The dashed lines are the representation of the Benzeggagh / Gong criterion (cf eq 7) [1] where the parameter $m = 8.9$ and 6.3 .

$$G_T = G_{I_{max}} + (G_{II_{max}} - G_{I_{max}}) \left(\frac{G_{II}}{G_T} \right)^m \quad (7)$$

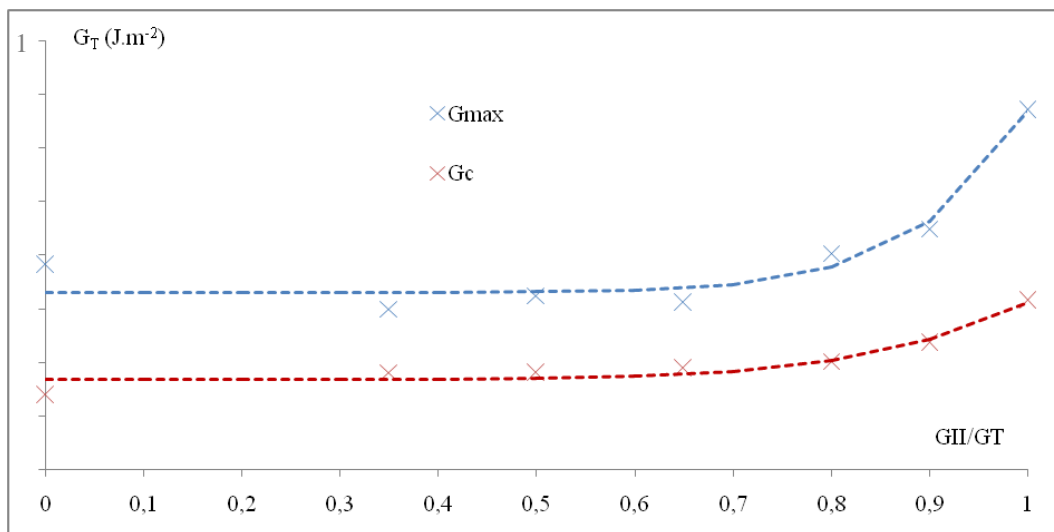


Figure 12. Evolution of critical and maximum energies release rates depending on the modal ratio

The evaluation of this criterion permits to feed models. They then will allow to make tests / calculations correlations to study the complex phenomena present during the propagation phase. With this in mind, Figures 13 to 15 show the evolution of deformations ϵ_x , ϵ_y and shear γ depending on the evolution of the modal ratio. These strain fields allow to calibrate the models.

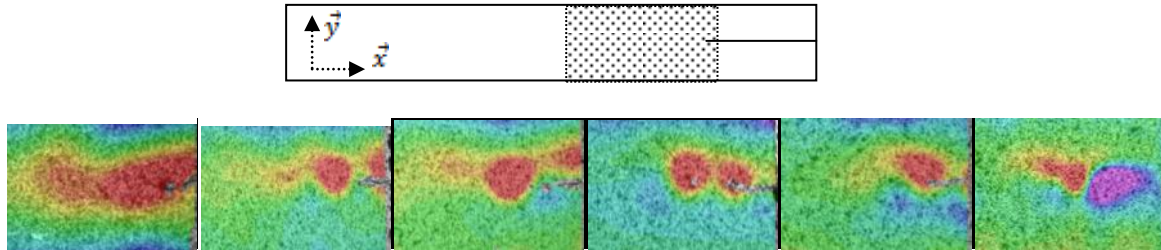


Figure 13. Evolution of deformation along x at microscopic initiation for the modals ratios (0, 0.35 0.65, 0.8, 0.9 and 1)

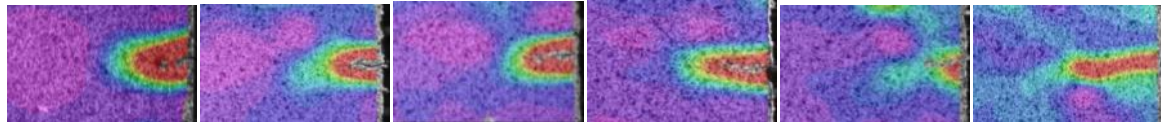


Figure 14. Evolution of deformation along y at microscopic initiation for the modals ratios (0, 0.35 0.65, 0.8, 0.9 and 1)

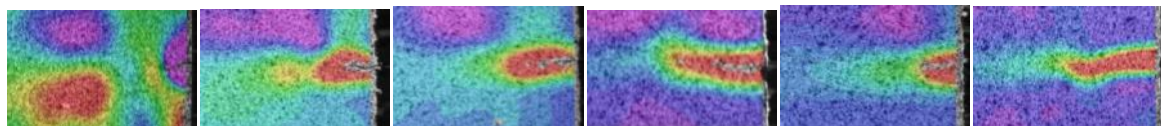


Figure 15. Evolution of shear at microscopic initiation for the modals ratios (0, 0.35 0.65, 0.8, 0.9 and 1)

4 Conclusion

This study highlights the importance of the choice of the specimens width. Indeed, the influence of edge effects is important in the case of 3D weaving.

Moreover, this work has allowed to refine a methodology for studying crack initiations for modes I, II and mixed. The detection of two types of initiations was made possible by the multiplication of measurement and observation means.

On the other hand, the propagation remains an open problem. The discontinuities in the propagation phases make difficult the determination of a energy release rate of propagation. Therefore, in a near future, testing/calculation correlations will be conducted to attempted to identify phenomena involved.

References

- [1] Benzeggagh M, Kenane M, Measurement of mixed-mode delamination Fracture toughness of unidirectional Glass/epoxy composites with mixed-mode Bending apparatus. *Composites science and technology*. 56:439-449 (1996)
- [2] ASTM D5528-01, *Standard Test Method for Mode I Interlaminar Fracture Toughness of Unidirectional Fiber-Reinforced Polymer Matrix Composites* (2007)
- [3] Reeder JR, Crews JH. Redesign of the mixed-mode bending delamination test to reduce non-linear effects. *Journal of composites technology and research*. 14:12-19 (1992)
- [4] Benzeggagh M, *Application de la mécanique de la rupture aux matériaux composites*. PhD thesis (1980)